SEDIMENTOLOGY the journal of the International Association of Sedimentologists IAS

Sedimentology (2012) doi: 10.1111/sed.12005

Association of phosphate with rhyolite glass in marine Neogene tuffs from Patagonia, Argentina

NORA RUBINSTEIN*, ANA M. FAZIO , ROBERTO A. SCASSO* and STEVEN CAREY
**Departamento de Geolog a, Pabellon 2, CONICET, Universidad de Buenos Aires, Ciudad Universitaria, CP 1428, Buenos Aires, Argentina (E-mail: nora@gl.fcen.uba.ar)*
Departamento de Geolog a, Pabellon 2, Ciudad Universitaria, Universidad de Buenos Aires, CP 1428, Buenos Aires, Argentina
Graduate School of Oceanography, University of Rhode Island, Narragansett Bay Campus, 02882, RI, USA

Associate Editor – Adrian Immenhauser

ABSTRACT

The precipitation/replacement of Ca-phosphate is a complex process that commonly takes place during the early diagenesis in marine sediments. The unusual occurrence of shallow marine, early diagenetic phosphatic deposits associated with glassy tuffs in the Neogene Gaiman Formation, in the Chubut Province, Patagonia, Argentina, constitutes a good case example for the study of replacement and precipitation of Ca-phosphate on an unstable substrate. Isocon diagrams illustrate that chemical changes during glass diagenesis include gains in loss on ignition and Ca, and losses of K. These changes are the result of glass hydration during sea water glass interaction, together with adsorption and diffusion of ions into the bulk shard; combined, these represent an incipient process of volcanic glass replacement by Ca-phosphate. Subsequent early diagenetic P enrichment in the pore solutions led to phosphate precipitation, associated with pitting on the glass shards and pumice. The associated development of a reactive surface promoted the incorporation of P and Ca into their margins. Lastly, precipitation of calcium phosphate filled the vesicles and other open cavities, inhibiting further glass dissolution. The high porosity and reactivity of the volcanic glass provided an appropriate substrate for phosphate precipitation, leading to the development of authigenic apatite concretions in the volcanic-glass bearing strata of the Gaiman Formation. This research is of significance for those concerned with marine phosphatic deposits and sheds light on the processes of early diagenetic phosphate precipitation by replacement of an atypical, unstable substrate like hydrated volcanic glass.

Keywords Gaiman Formation, phosphate, phosphogenesis, tuffs, volcanic glass.

INTRODUCTION

The processes of concentration and precipitation/replacement of phosphate in diagenetic marine environments are of general significance for current understanding of the global phosphorous cycle (Follmi, 1996). Replacement is a complex process which is not well-understood yet, and most examples in the literature refer to Ca-phosphate replacement of calcium carbonate substrates (Prevot & Lucas, 1986; Lamboy, 1993). Case examples of phosphate precipitation associated with other types of substrates are uncommon. The present study

took advantage of a rare type of phosphate concretion developed on vitric, non-welded tuffs interbedded in the shallow marine Neogene sequence of the Gaiman Formation (Leanza *et al.*, 1981; Scasso & Castro, 1999), in order to investigate the processes of concentration and precipitation/replacement of phosphate. Textural changes, together with the novel use of isocon diagrams, allowed an assessment of subtle trace element changes in glass particles prior to and during phosphate precipitation.

Phosphogenesis in association with volcanic products has rarely been reported in the scientific literature and, when integrated over geological time, volcanic activity seems to represent a negligible source of phosphate (Föllmi, 1996). In spite of that, Ca-phosphate precipitated and replaced the siliceous glassy particles in the tuffs of the Gaiman Formation. Because siliceous volcanic glass is poor in phosphorus, an external source of phosphorus was needed.

Calcium-phosphate precipitation commonly takes place either directly, through nucleation and crystallization on mineral surfaces or biological webs, or through dissolution/precipitation replacement of existing minerals, in most cases calcium carbonates (Prevot & Lucas, 1986; Lamboy, 1990, 1993). Initial hydration and enrichment of Ca and P was followed by massive precipitation of Ca-phosphate on the surface of glassy particles of the Gaiman Formation, providing a good example of how the replacement processes proceed on unstable, amorphous materials and how they stop. Once formed, the Ca-phosphate nuclei usually serve as a template for further phosphate accretion, until interstitial dissolved phosphate levels are too low to sustain further precipitation (Van Cappellen, 1991) or until levels of alkalinity are high enough to prevent further Ca-phosphate precipitation (Baturin & Savenko, 1985; Glenn *et al.*, 1988). However, the importance of hydration on the substrate typically has not been considered. Hydration of volcanic glass played a critical role in glass dissolution and phosphate precipitation in the Gaiman Formation tuffs. In addition, Ca-phosphate precipitation itself may stop the replacement process by preventing fluid circulation into the pores. This article serves to provide insight into an unrecognized style of phosphate precipitation, drawing attention to a process that has not been previously recognized in the literature.

GEOLOGY OF THE STUDY AREA

The Gaiman Formation is the formal name (Mend a & Bayarsky, 1981) for the Lower Miocene 'Patagoniense' in the region of the Lower Valley of the Chubut River. The Gaiman Formation is a 90 m thick clastic marine unit, part of the classical Cenozoic sequence cropping out in the vicinity of the city of Gaiman, Chubut Province, Patagonia, Argentina (Fig. 1). The Gaiman Formation was deposited in a shallow-marine environment (Scasso *et al.*, 1996; Scasso & Castro, 1999) and consists of a coarsening-upward succession of poorly consolidated mudstones, tuffs, sandstones and coquinas (Fig. 1). The lower part of the unit consists largely of tuffaceous bioturbated mudstones, with remains of marine vertebrates, and rare levels of the mollusc *Ostrea*. The upper part is composed mainly of sandstones, tuffaceous sandstones and interbedded mudstones. Well-preserved *Ophiomorpha* burrows are typical in this part of the section. The presence of abundant fresh and slightly reworked volcanic glass (Mend a & Bayarsky, 1981) indicates a dominant provenance from contemporaneous volcanic products for the clastic sediments. Subordinate sources were the tuff deposits of the underlying Sarmiento Formation, the Upper Jurassic volcanic succession and crystalline basement that crop out in the area (Scasso & Castro, 1999).

PHOSPHATIC HORIZONS AND PHOSPHOGENESIS

Thin phosphatic horizons occur sporadically throughout the Gaiman Formation (Fig. 1). Two types of phosphatic horizons are recognized (Scasso & Castro, 1999): 'Type 1' consists of *in situ* concretions about 10 cm in diameter, dispersed in the host sediments, usually tuffaceous sandy mudstones, wackes or tuffs. These deposits were interpreted by Scasso & Castro (1999) as condensed beds associated with long periods of slow sedimentation, part of transgressive to early highstand system tracts. 'Type 2' phosphates are related to autochthonous reworking, winnowing and mechanical concentration of resistant particles. Phosphatic remains, such as bones, teeth and concretions, along with abraded shells and pebbles, are found embedded in a sandy matrix. A number of these horizons are considered to be reworked horizons associated with transgressive surfaces.

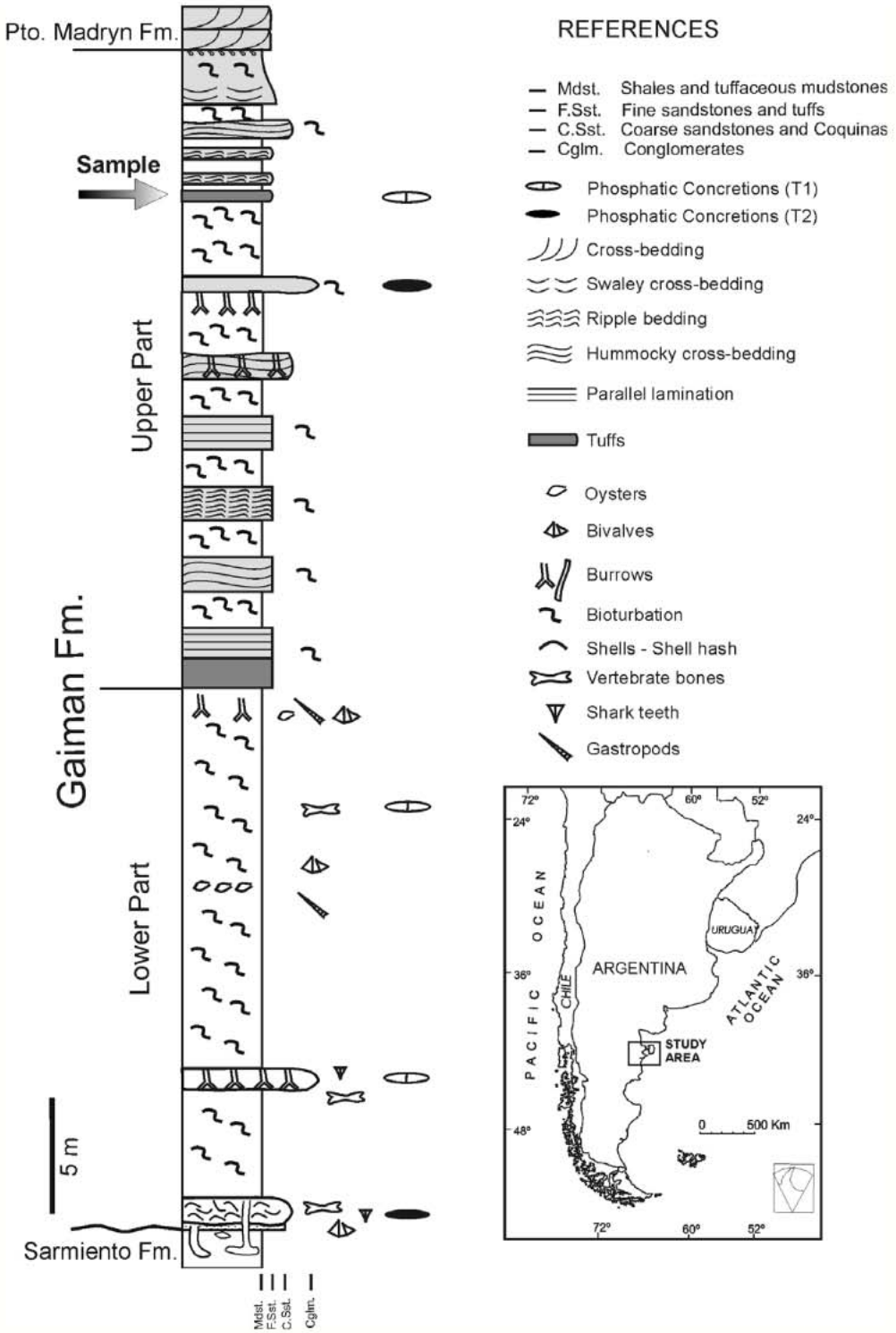

Fig. 1. Location map and schematic log of the Gaiman Formation showing the stratigraphic position of the analysed sample.

Phosphatic nodules show P_2O_5 contents between 15 6 wt% and 21 8 wt% (Scasso & Castro, 1999). The phosphate is constituted of tiny crystals <3 μm in diameter and very regular in size cementing organic phosphatic and non-phosphatic particles. X-ray diffraction analyses indicate that the crystals consist mainly of carbonate fluorapatite (Scasso & Castro, 1999).

The formation of marine phosphate deposits normally occurs just below the water sediment interface (a few centimetres to tens of centimetres), in a broadly suboxic environment, by means of P concentration in pore waters and phosphate precipitation (Jarvis *et al.*, 1994). Main sources of sedimentary phosphate are the microbial breakdown of buried organic matter and redox-driven phosphate desorption from iron and manganese oxyhydroxides (Follmi, 1996), even though dissolved sea-water phosphate represents an additional source which may become locally important. In the tuffs, P is sourced from organic matter decomposition and also by Fe and Mn oxy-hydroxy complexes. Recurrent changes in the oxidation states of Fe and Mn can promote phosphate precipitation (Froelich *et al.*, 1988; Glenn & Arthur, 1990). When Fe III and Mn IV colloids precipitate, they scavenge soluble phosphate from sea water to form oxy-hydroxy complexes incorporated into the sediments. Redox conditions typically change from oxidizing to reducing during sediment burial, therefore promoting Fe and Mn reduction to soluble states and releasing P, from which phosphate minerals may be precipitated. This process, enhanced by water circulation through burrows at the Miocene sea water sediment interface, was responsible for the formation of Gaiman concretions (Scasso & Castro, 1999; Fazio *et al.*, 2007). Improved ion diffusion and pore water renewal in the sediments resulted in a widened oxic suboxic zone. In addition, sediment mixing and reworking by organisms, and micro-environments from organic matter decay within fossils and burrows, contributed to phosphatic concretion formation. Rare earth element patterns in early diagenetic concretions of the Gaiman Formation suggest quantitative precipitation from early diagenetic pore waters, reproducing the flat pattern of oxic suboxic recent pore waters (normalized to PAAS), which result from remineralization of organic coatings rich in Ce and other light rare earth elements (Fazio *et al.*, 2007).

ANALYTICAL TECHNIQUES

A sample of a 'Type 1' concretion was selected for geochemical glass shard analyses using a JEOL-JXA 50A microprobe (JEOL Ltd., Tokyo, Japan), operating at 10 nA beam current, five micrometre beam diameter, and 15 kV of accelerating voltage at the Department of Geology, Brown University. Sodium loss during analysis was calculated using a decay technique (Nielsen & Sigurdsson, 1981) by counting on sample for a

Table 1. Electron microprobe analyses of 20 glass shards from a sample of a phosphatic tuff from the Gaiman Formation. Measurements at different points of a single glass shard yielded almost identical results. Values in the table are the average of at least three measurements. The difference between the sum of the analyses and 100% is considered as the loss on ignition (LOI).

Shard	(%) SiO_2	(%) TiO_2	(%) Al_2O_3	(%) Fe_2O_3	(%) MnO_2	(%) MgO	(%) CaO	(%) Na_2O	(%) K_2O	(%) P_2O_5	(%) LOI(*)
S 1	69 99	0 23	12 21	1 15	0 04	0 24	1 36	3 51	3 36	0 05	7 88
S 2	71 66	0 25	10 97	1 35	0 06	0 22	1 38	3 84	2 27	0 01	7 99
S 3	70 24	0 18	11 94	2 03	0 05	0 12	1 27	3 57	3 67	0 01	6 92
S 4	72 70	0 12	12 18	1 24	0 10	0 06	0 62	4 02	3 92	0 01	5 04
S 5	71 79	0 23	11 14	1 29	0 02	0 17	1 01	2 99	3 28	0 00	8 07
S 6	73 81	0 07	11 89	0 83	0 11	0 15	0 93	2 89	3 55	0 04	5 73
S 7	75 01	0 08	12 05	1 60	0 03	0 00	0 18	3 68	4 81	0 01	2 54
S 8	73 65	0 25	11 35	1 68	0 05	0 24	1 69	3 50	1 38	0 07	6 13
S 9	70 54	0 11	12 06	2 11	0 09	0 12	1 80	4 31	2 12	0 04	6 70
S 10	68 89	0 29	12 43	2 13	0 08	0 24	1 44	4 42	3 03	0 04	7 00
S 11	68 13	0 22	12 23	2 38	0 06	0 23	1 95	3 33	3 07	0 04	8 36
S 12	70 33	0 26	12 03	1 87	0 10	0 21	1 41	4 52	2 47	0 03	6 78
S 13	72 21	0 08	11 48	1 47	0 07	0 00	0 35	4 30	4 53	0 02	5 49
S 14	70 75	0 07	12 17	1 00	0 12	0 08	0 76	4 17	3 69	0 05	7 12
S 15	71 62	0 25	11 12	1 81	0 10	0 26	1 72	4 36	1 61	0 04	7 09
S 16	72 46	0 16	11 40	1 75	0 04	0 18	1 48	3 98	2 40	0 04	6 11
S 17	71 81	0 23	11 47	1 31	0 09	0 19	1 11	3 69	3 63	0 03	6 43
S 18	71 27	0 16	11 44	1 92	0 06	0 07	1 12	4 31	2 96	0 01	6 67
S 19	73 10	0 18	11 26	1 42	0 07	0 11	1 03	4 29	2 91	0 02	5 56
S 20	71 88	0 12	11 60	1 14	0 03	0 08	0 9	3 39	4 10	0 04	6 71

10 sec period, determining the rate of Na loss from the counts and then extrapolating back to zero time to get the initial Na content. Average values of three consistent measurements at different points inside a single shard are shown in Table 1. During the microprobe sessions the KN-18 obsidian glass standard was measured several times. Standard deviation for elements above 1% of the sample was always below 5% and maximum error in individual measurements was always below 15% of the 'true' value published. A systematic shift with time in the SiO_2 and Al_2O_3 values of <2% was corrected using appropriate software algorithms and LOI (loss on ignition) values were estimated by using the difference between 100% and the sum of microprobe data. Glass surfaces were observed in polished, uncovered sections under a scanning electron microscope (JEOL JSM 5900LV) and semi-quantitative energy dispersive spectrometer (EDS) analyses were carried out with a PGT EDS system.

RESULTS

Petrography

The concretion is developed within a vitric tuff that consists mainly of fresh, colourless, cuspate or platy glass shards and pumice with minor crystals and lithoclasts. Crystals mainly consist of quartz with minor biotite, feldspar, pyroxene and amphibole (Fig. 2). Biotite appears slightly altered to white mica, along with opaque minerals, and phosphate growth is observed between flakes. Feldspars are fresh and usually show polysynthetic twinning. Completely sericitized crystals, probably from feldspars, are also recognized. Lithoclasts are composed mainly of volcanic rocks with a felsitic to granophyric and pilotaxic texture, with minor occurrence of quartz-sericite aggregates; they are partially replaced by phosphate (Fig. 3). Pellets are common. Calcite clusters and epidote grains are also recognized. The matrix has mostly been replaced by tiny (<3 μm) phosphate crystals but some small glass, crystal and lithic particles still remain (Fig. 3). Single phosphate crystals show an elliptical to roughly cubic shape, often with a trough or a groove-like depression in their centre (Fig. 4A to C); sometimes they exhibit more regular crystal faces (Fig. 4D). Individual or clustered phosphate crystals have also grown within biotite flakes and pumice vesicles. Phosphate replacements along the shard walls are non-pseudomorphic (Figs 3 and 4A). Vesicles may also be filled with clay minerals (Fig. 3). The surface of the glass looks corroded and partially dissolved with some pitting that produced a spongy texture (Fig. 4B to D).

Chemical composition

Table 1 shows major element data determined by electron microprobe on 20 glass shard samples. Fluorine contents were below detection

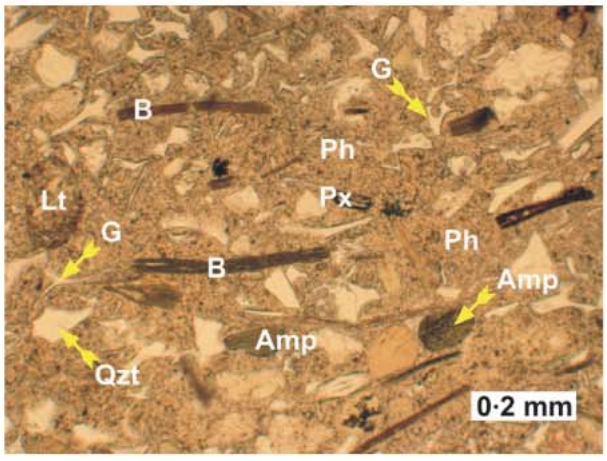

Fig. 2. Microphotograph of a thin section showing phosphatic cement 'Ph', glass shards 'G', lithics 'Lt', amphibole 'Amp', quartz 'Qtz', biotite 'B' and pyroxene 'Px' crystals.

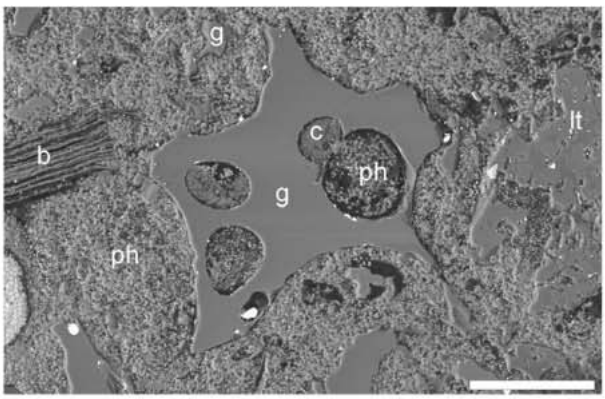

Fig. 3. Back-scattered SEM picture of a glass shard in a phosphatic matrix. Tiny phosphate crystals of similar size make up most of the background and grow inside the vesicles 'ph', sometimes together with clay minerals 'c'. Phospate also grows inside biotite flakes 'b' replaces part of a lithic fragment 'lt' and most of the matrix, where some small glass particles 'g' still remain. Scale bar 20 microns long.

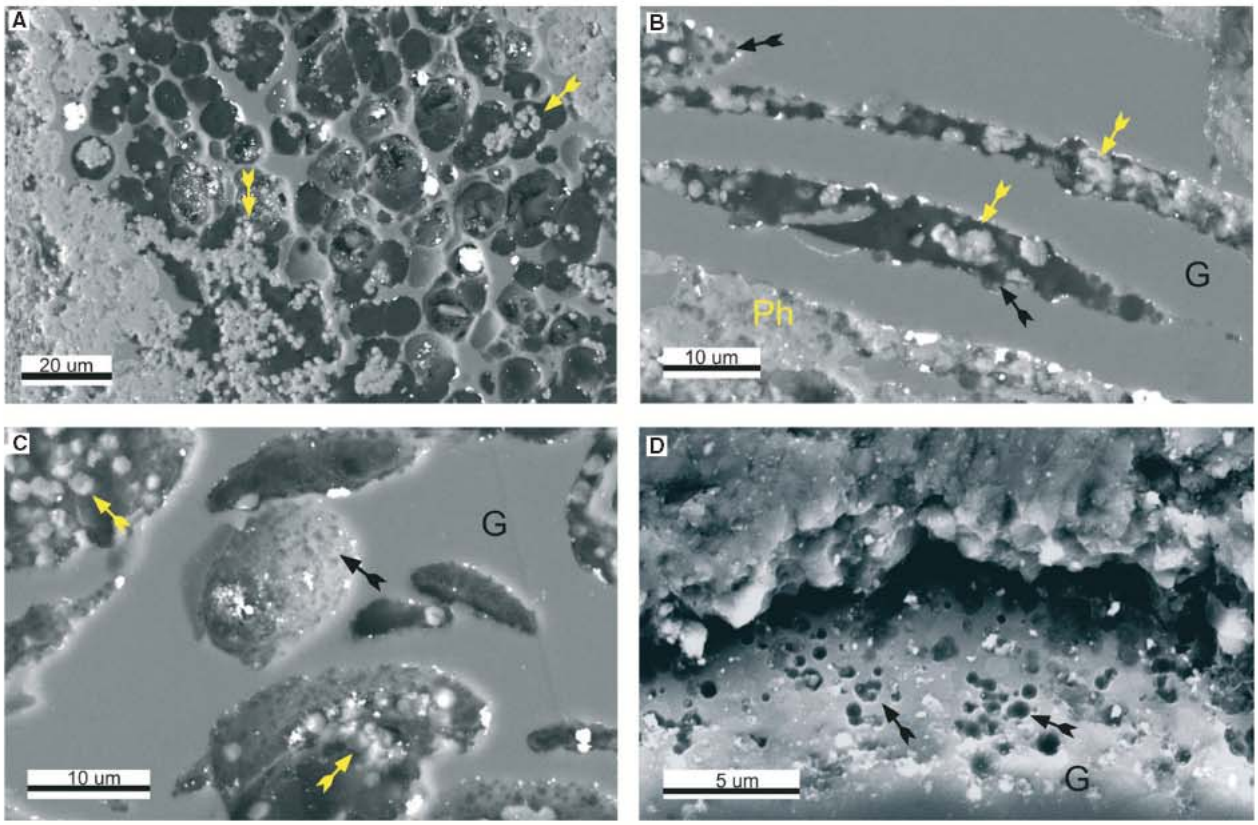

Fig. 4. (A) Back-scattered SEM image of a pumice fragment surrounded and partially replaced by phosphate. Vesicles are mostly empty but some of them are partially filled by small phosphate crystals (yellow arrows) with a roughly cubic shape and a trough in their centre. (B) and (C) Similar to (A) but pitting and dissolution along the glass margins and vesicle walls are shown (black arrows). 'Ph' phosphatic cement, 'G' glass shards. (D) Scanning electron microscope image showing drusy phosphate crystals with more regular crystal faces when growing along the open spaces.

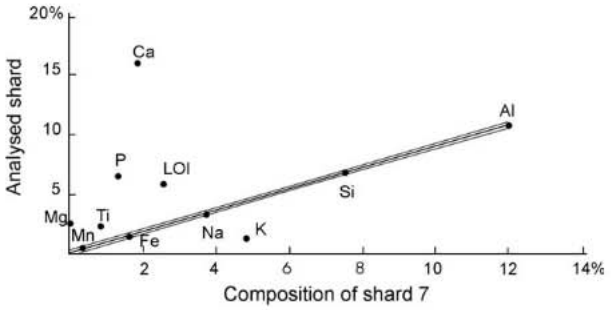

Fig. 5. Isocon diagram for shard 8 in Table 1. All of the samples were plotted against sample 7, the one with the lowest loss on ignition (LOI) which was considered to be the less altered sample. Oxide percentages have been scaled for a suitable representation with the following factors: SiO_2/10; MgO*20; P_2O_5*1; CaO*20; TiO_2*30; MnO*30; LOI*2. Dotted line indicates the 95% confidence band.

limit in all the analysed samples. Chemical compositions of the glass shards indicate that they correspond to rhyolitic compositions according to the TAS (total alkalis versus silica) classification (Le Maitre *et al.*, 1989).

Isocon diagrams (Grant, 1986) were used in order to establish changes in major element content produced by alteration processes (Fig. 5). This graphical method is usually applied to determine the relative gains and losses of elements from chemical analyses of altered and unaltered (or less altered) equivalents in rocks, as a result of hydrothermal alteration processes. When a linear relation of some elements is obtained by plotting the analytical data of the altered against the unaltered rock, it may be assumed that they have been immobile during the alteration process. As an unaltered sample is lacking, it was assumed that the shard sample with the lowest degree of hydration, indicated by the lowest LOI content (in this case sample 7), is the least altered compared with the protolith. The scaled amounts of the different elements in every sample and the same elements in sample 7 are plotted in Fig. 5. Silicon, Al and Fe show a good linear array. Sodium and Mn plot very close or inside the 95% confidence band. Potassium always plots below the

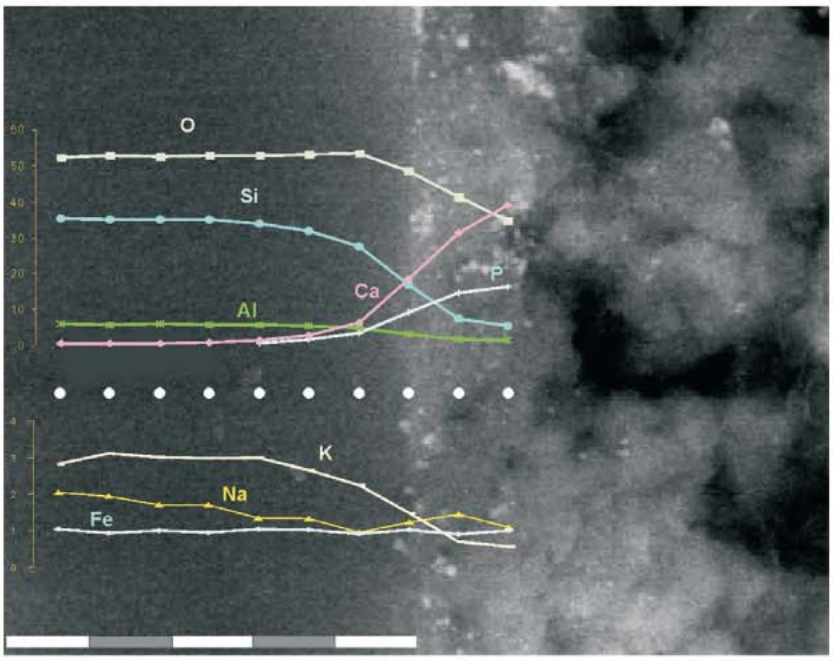

Fig. 6. Back-scattered SEM image showing variation in element contents across the contact between a glass shard and the phosphatic cement. Location of the points where the beam was focused is shown with white circles: O, Si, Al and K strongly decrease, Na and Fe do not change and Ca and P increase from the glass to the phosphate. A closer look shows relative oxygen enrichment and Na loss at the glass margin. Loss of Si and K, as well as gain of Ca and P, start beyond the influence of the beam radius (about 1 micron). Scale bar 5 microns long.

confidence band, whereas LOI, Ca, Mg, Ti and frequently P plot above the band.

Detailed observation with EDS at the wall of the glass in contact with Ca-phosphate shows maximum O and minimum Na at the contact (Fig. 6). Towards the margin of the shard and into the phosphate Ca and P are enriched, whereas Si, Al and K decrease and Fe content is uniform.

DATA INTERPRETATION

The isocon diagrams (Fig. 5) show the best linear array for Si, Al and Fe, so it can be assumed that no significant gains and losses of these elements, which are generally known to be immobile under these conditions, occurred in the inner part of the shard. Sodium plots very close to or inside the 95% confidence band, so this implies that it had almost no gains or losses either. Elements present in very small amounts (<<1%; Mg, Ti, Mn and P) are not considered for the analysis, due to the higher uncertainty of the microprobe analysis. Potassium always plots below the confidence band indicating that there were absolute losses of this element, whereas gains in LOI and Ca are indicated by plots above the band.

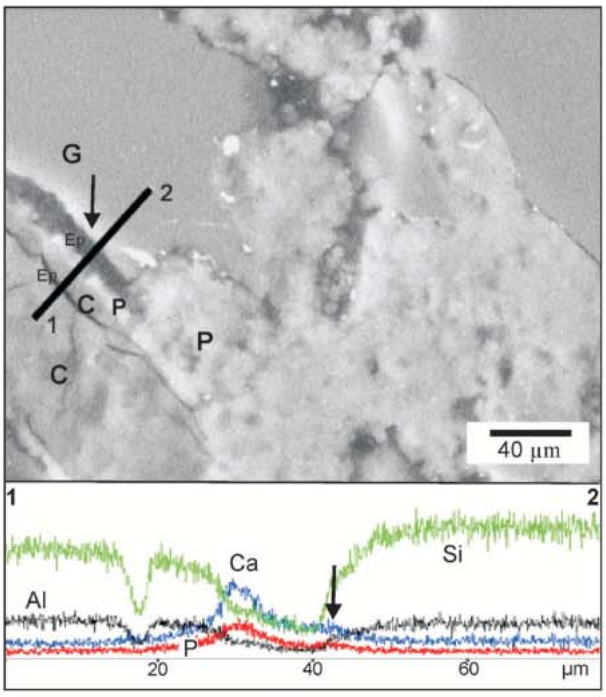

Fig. 7. Back-scattered SEM image and line spectrum (1–2). A clay mineral 'C', the phosphatic cement 'P', empty pores ('Ep', shadow) and a glass shard 'G' are included in the line spectrum, which shows the relative contents of Si, Al, Ca and P. Note the Ca and minor P increase (arrowed) in the inner border of the glass particle.

Replacement of glass by phosphate is non-pseudomorphic, that is to say this is not a molecule by molecule replacement but glass dissolution shortly preceded phosphate precipitation. Small-scale pitting produced irregular outlines and engulfments along the walls of the shards and in the inner walls of the vesicles (Fig. 4B to D) suggesting that glass shards underwent extensive dissolution prior to massive phosphate precipitation in the voids. Glass dissolution was probably partially synchronous with incipient phosphate precipitation during the early diagenesis. Small individual or clustered phosphate crystals grew attached to the walls of the cavities in the pumice. Precipitation and moulding of empty spaces seem to be a common process that may predominate over real replacement (Lamboy, 1990). The small size of the crystals is due to the growth kinetics (Van Cappellen, 1991; Van Cappellen & Berner, 1991).

Most of the phosphate crystals in the Gaiman Formation are morphologically similar to microbial biostructures (Soudry, 1992, 2000; Baturin, 2000; Thorseth *et al.*, 2003) that also commonly show a central void, although similar structures may be also precipitated under sterile conditions (Van Cappellen, 1991). Some crystals in Gaiman Formation tuffs show incipient plane faces (Fig. 4D), probably developed shortly after precipitation, because on a time scale of 10 to 100 years after precipitation francolite attains a better crystallinity (Gulbrandsen *et al.*, 1984; Jarvis *et al.*, 1994; Follmi, 1996).

Bacterial precipitation of Ca-phosphates seems to be a rather common phenomena forming micron or submicron size microstructures in other geological sequences (e.g. Benzerara *et al.*, 2004) and probably is due to the increasing P concentration in pore solutions. At the same time, marine micro-organisms can also be highly efficient in promoting glass dissolution (Brehm *et al.*, 2005). In the open early diagenetic system, Ca is sourced from sea water or by dissolution of calcitic shells from the sediments.

Calcium-phosphorus increase and Si–Al–K decrease observed in EDS analyses towards the margin of the shard and into the phosphate might be an artifact caused by the diameter of the EDS beam (*ca* 2 μm). However, these trends start inside the shards several microns from the margin; therefore, they must truly reflect replacement processes. On the other hand, the walls of glass shards facing empty spaces (Fig. 7) show Ca and slight P enrichment in the outermost part of the shard. Calcium and P were incorporated into the margins of the shards, as demonstrated by the EDS analysis, but isocon results also suggest Ca incorporation into the whole body of the shards.

DISCUSSION

Losses in K and gains in volatiles (LOI) and Ca are interpreted to reflect glass hydration that occurs in the whole body of the shard, caused by the interaction of the glass with sea water during deposition, and thereafter with pore water during early diagenesis. It is believed that hydration was crucial for further diagenetic processes. Hydration is associated with structural changes, like hydrolysis of an activated surface complex: $Si(OH)_3$ (Grambow, 1992); deprotonation of terminal Si or Al sites (Brady & Walther, 1992); or nucleofilic attack by OH^- at Si sites (Kubicki *et al.*, 1993). Thus, hydrolysis of bounded Al and Si tetrahedron occurs, and this is a network-opening reaction (Hamilton *et al.*, 2001) which allows volume increase, and the diffusion and introduction of metals into the glass structure.

Laboratory results related to the alteration of glass in an aqueous medium (Doremus, 1994) indicate that the process begins with an attack on the more labile functional groups in contact with the solvent. This implies surface retention of H^+ ions in an acid medium, or OH in an alkaline medium like the sea water, and the consequent increase in O content at the borders of the shard. The retained surface OH group has donor properties and may form surface complexes with metals in solution:

S OH Me SO – Me
H S- represents surface sites

The sorption of metals takes place at specific surface coordination sites and surface charge results from the sorption reaction (Dzombak & Morel, 1990). For alkali and earth alkali cations the tendency to become sorbed increases with the ionic radius (Stumm & Morgan, 1996):

Rb > K > Na > Li relative orderings of ionic radii

Ba > Sr > Ca > Mg relative orderings of ionic radii

In sea water, Ca and Na are preferentially adsorbed compared with Mg and K, and thus local increases of Ca and Na occur at the glass

surface. Following the Goldschmidt Rules that describe partitioning of trace elements between solids and melt according to their ionic radius and charge, the smaller and higher charge ions will replace the larger and lower charge ones (White, 2005). Thus, Ca^{2+} (ionic radius 1 00 A) exchanges with K^{+} (ionic radius 1 38 A) and Na^{+} (ionic radius 1 02 A). The chemical changes in the composition of the altered glass reflect these types of replacements of K by Ca that take place together with the hydration of the glass, or of Na by Ca at the margins of the shards. If phosphate is abundant in the aqueous solution, competitive complex surface solution reaction for Ca may occur in the reactive surface of the shard (Fig. 6). Therefore, nucleation and growth of phosphate are favoured by shards undergoing dissolution, via complex surface solution reactions. A similar mechanism involving adsorption of calcium at the Si-surface group followed by attachment of the HPO_4 was proposed for Ca-phosphate nucleation at silica surfaces (Sahai, 2003). Thus, the shards represent a suitable substrate for the development of authigenic phosphate. Phosphate formed at the shard margins stabilized the glass margin stopping dissolution and pitting (for example, Fig. 7). If the concentration of the soluble Ca-phosphate complex exceeds its solubility product, massive precipitation of calcium phosphate occurs around the glass shards. In that case, Ca-phosphate crystals fill the vesicles and pores excluding the glass surface from further contact with sea water and inhibiting glass dissolution.

CONCLUSIONS

Analyses of chemical and textural changes of the glass shards in the Neogene Gaiman Formation of Argentina allow the study of early diagenetic glass hydration, dissolution and phosphogenetic processes. A model is developed for sequential changes to rhyolite glass that promote the formation of phosphate nodules. Initially, glass hydration due to sea water glass interaction and chemical changes due to adsorption and diffusion of ions into the bulk shard triggers volcanic glass replacement. During this process, P enrichment in the pore solutions occurs simultaneously, with pitting dissolution and the development of a reactive surface that promotes the incorporation of P and Ca in the shard margins. Based on the Goldschmidt Rule, increased concentrations of Ca on grain surfaces facilitates phosphate mineralization on such Ca-enriched surfaces. After P and Ca enrichment, shard margins becomes stabilized, dissolution stops and massive precipitation of calcium phosphate eventually takes place at the margins of the shards or filling the open pore cavities. This precipitation inhibits further fluid-driven glass dissolution processes. The study demonstrates that non-welded tuffs provide an appropriate substrate for phosphate precipitation during early diagenesis, due to the high reactivity and porosity of the volcanic glass. When early diagenetic phosphate precipitation 'freezes' the degradation of these glassy volcanic sediments amid their breakdown, it provides a preservational window through which diagenesis of volcaniclastic sediments can be better observed.

ACKNOWLEDGEMENTS

Joe Devine (Brown University) provided invaluable assistance and expertise during microprobe analyses. We thank John Compton and two anonymous reviewers for constructive reviews of the manuscript. Funding by UBACYT, CONICET and Fulbright Foundation is greatly acknowledged.

REFERENCES

Baturin, G.N. (2000) Formation and evolution of phosphorite grains and nodules on the Namibian Shelf, from Recent to Pleistocene. In: *Marine Authigenesis, from Global to Microbial* (Eds C. Glenn, L. Prevot Lucas and J. Lucas), SEPM Spec. Publ., **66**, 185 200.

Baturin, G.N. and **Savenko, V.S.** (1985) Mechanism of formation of phosphorite nodules. *Oceanology*, **25**, 747 750.

Benzerara, K., Menguya, N., Guyota, F., Skouria, F., de Lucab, G., Barakatb, M. and **Heulinb, T.** (2004) Biologically controlled precipitation of calcium phosphate by *Ramlibacter tataouinensis*. *Earth Planet. Sci. Lett.*, **228**, 439 449.

Brady, P.V. and **Walther, J.V.** (1992) Surface chemistry and silicate dissolution at elevated temperatures. *Am. J. Sci.*, **29**, 639 658.

Brehm, U., Gorbushina, A. and **Mottershead, D.** (2005) The role of microorganisms and biofilms in the breakdown and dissolution of quartz and glass. *Palaeogeogr. Palaeoclimatol. Palaeoecol.*, **219**, 117 129.

Doremus, R. H. (1994) Chemical durability: reaction of water with glass. In: *Glass Science* (Ed. R.H. Doremus), pp. 215 240. John Wiley & Sons, New York.

Dzombak, D.A. and **Morel, F.M.** (1990) *Surface Complexation Modeling: Hydrous Ferric Oxide*. Wiley-Interscience, New York, 393pp.

Fazio, A.M., Scasso, R.A., Castro, L.N. and **Carey, S.** (2007) Geochemistry of rare earth elements in early-diagenetic miocene phosphatic concretions of Patagonia, Argentina: phosphogenetic implications. *Deep-Sea Res. II*, **54**, 1414 1432.

Follmi, K.B. (1996) The phosphorus cycle, phosphogenesis and marine phosphate-rich deposits. *Earth-Sci. Rev.*, **40**, 55 124.

Froelich, P., Arthur, M.A., Burnett, W., Deakin, M., Hensley, V., Jahnke, R., Kaul, L., Kim, K., Roe, K., Soutar, A. and **Vathakanon, C.** (1988) Early diagenesis of organic matter in Peru continental margin sediments: phosphorite precipitation. *Mar. Geol.*, **80**, 309 343.

Glenn, C.R. and **Arthur, M.A.** (1990) Anatomy and origin of a Cretaceous phosphorite-greensand giant, Egypt. *Sedimentology*, **37**, 123 154.

Glenn, C.R., Arthur, M.A., Yeh, H.W. and **Burnett, W.C.** (1988) Carbon isotopic composition and lattice-bound carbonate of Peru-Chile margin phosphorites. In: *The Origin of Marine Phophorite. The Results of the R.V. Robert D. Conrad Cruise 23-06 to the Peru Shelf* (Eds W.C. Burnett and P.N. Froelich), Mar. Geol., **80**, 287 307.

Grambow, B. (1992) Geochemical approach to glass dissolution. In: *Corrosion of Glass, Ceramics and Ceramic Superconductors* (Eds D.E. Clark and B.K. Zoitos), pp. 124 152. Noyes Publications, Noyes editions Park Ridge, USA.

Grant, J.A. (1986) The isocon diagrams a simple solution to Gresen's equation for metasomatic alteration. *Econ. Geol.*, **81**, 1976 1982.

Gulbrandsen, R.A., Roberson, C.E. and **Neil, S.T.** (1984) Time and the crystallization of apatite in seawater. *Geochim. Cosmochim. Acta*, **48**, 213 218.

Hamilton, J.P., Brantley, S., Pantano, C.G., Criscenti, L.J. and **Kubicki, J.D.** (2001) Dissolution of nepheline, jadeite and albite glasses: toward better models for aluminosilicate dissolution. *Geochim. Cosmochim. Acta*, **65**, 3693 3702.

Jarvis, I., Burnett, W., Nathan, J., Almabaydin, F., Attia, A., Castro, L., Husain, V., Qutawwna, A., Sejani, A. and **Zanin, Y.** (1994) Phosphorites geochemistry: state of the art and environmental concerns. *Eclogae Geol. Helv.*, **87**, 643 700.

Kubicki, J.D., Xiao, Y. and **Lasaga, A.C.** (1993) Theoretical reaction pathways for the formation of [Si(OH)5]1 and the deprotonation of orthosilicic acid in basic solution. *Geochim. Cosmochim. Acta*, **57**, 3847 3853.

Lamboy, M. (1990) Microstructures of a phoshphatic crust from the Peruvian continental margin: phosphatized bacteria and associated phenomena. *Oceanol. Acta*, **13**, 439 451.

Lamboy, M. (1993) Phosphatization of calcium carbonate in phosphorites: microstructures and importance. *Sedimentology*, **40**, 53 62.

Le Maitre, R.W., Bateman, P., Dudek, A., Keller, J., Lameyre, P., Le Bas, M.J., Sabine, P.A., Schmid, R., Sorensen, H., Streckeisen, A., Woolley, A.R. and **Zanettin, B.** (1989) *A Classification of Igneous Rocks and Glossary of Terms. Recommendations of the IUGS Subcommission on the Systematics of Igneous Rocks*. Blackwell, London, 204 pp.

Leanza, H.A., Spiegelman, A.T. and **Hugo, C.A.** (1981) Manifestaciones fosfaticas de la Formacion Patagonia: su genesis y relacion con el vulcanismo piroclastico silíceo. *Rev. Asoc. Argentina Mineral. Petrol. Sedimentol.*, **11**, 1 12.

Mend a, J.E. and **Bayarsky, A.** (1981) Estratigrafía del Terciario del valle inferior del río Chubut. *8th Congreso Geologico Argentino, San Luis*, **3**, 593 603.

Nielsen, C. and **Sigurdsson, H.** (1981) Quantitative methods for electron microprobe analyses of sodium in natural and synthetic glasses. *Am. Mineral.*, **66**, 547 552.

Prevot, L. and **Lucas, J.** (1986) Microstructure of apatite replacing carbonate in synthesized and natural samples. *J. Sed. Petrol.*, **56**, 153 159.

Sahai, N. (2003) The effects of Mg2+ and H+ on apatite nucleation at silica surfaces. *Geochim. Cosmochim. Acta*, **67**, 1017 1030.

Scasso, R.A. and **Castro, L.N.** (1999) Cenozoic phosphatic deposits in North Patagonia, Argentina: phosphogenesis, sequence-stratigraphy and paleoceanography. *J. South Am. Earth Sci.*, **12**, 471 487.

Scasso, R.A., Castro, L.N., Lippai, H. and **Alonso, M.S.** (1996) Significado estratigrafico y paleoambiental del conglomerado fosfatico "Patagoniense" del Bryn Gwyn, Gaiman (provincia de Chubut). *6th Reunion Argentina Sedimentolog a, Bahia Blanca, Actas*, **1**, 117 122.

Soudry, D. (1992) Primary bedded phosphorites in the Campanian Mishash Formation, Negev, southern Israel. *Sed. Geol.*, **80**, 77 88.

Soudry, D. (2000) Carbonate-phosphate competition in the Negev phosphorites (Southern Israel): a microstructural study. In: *Marine Authigenesis, From Global to Microbial* (Eds C. Glenn, L. Prevot Lucas and J. Lucas), *SEPM Spec. Publ.*, **66**, 415 426.

Stumm, W. and **Morgan, J.J.** (1996) *Aquatic Chemistry, Chemical Equilibria and Rates in Natural Waters*, 3rd edn. John Wiley & Sons Inc., New York, 1022 pp.

Thorseth, H.I., Pedersen, R.B. and **Christie, D.M.** (2003) Microbial alteration of 0 30-Ma seafloor and sub-seafloor basaltic glasses from the Australian Antarctic Discordance. *Earth Planet. Sci. Lett.*, **215**, 237 247.

Van Cappellen, P. (1991) *The formation of marin apatite. A kinetic study*. Unpublished PhD thesis, University of Yale, New Haven, CT, USA, 240 pp.

Van Cappellen, P. and **Berner, R.A.** (1991) Fluorapatite crystal growth from modified seawater solutions. *Geochim. Cosmochim. Acta*, **55**, 1219 1234.

White, W.M. (2005) *Geochemistry*. John Hopkins University Press, Baltimore, 700 pp.

Manuscript received 24 November 2011; revision accepted 24 October 2012